



# Polyether-block-amide thin-film composite hollow fiber membranes for the recovery of butanol from ABE process by pervaporation

Carla Arregoitia-Sarabia, Daniel González-Revuelta, Marcos Fallanza, Alfredo Ortiz, Daniel Gorri\*

Departamento de Ingenierías Química y Biomolecular, Universidad de Cantabria, Av. de Los Castros s/n, 39005 Santander, Spain

## ARTICLE INFO

### Keywords:

Hollow fiber membranes  
Selective membranes  
Pervaporation  
Biobutanol recovery  
Biofuels

## ABSTRACT

This work reports the continuation of previous efforts to recover butanol from the ABE (acetone-butanol-ethanol) fermentation process by pervaporation (PV). A key aspect to improve the efficiency of the technology is the membrane used to perform the selective butanol separation; hence, this study focuses on the implementation of hollow fiber (HF) membrane configuration for the ABE separation by PV as opposed to flat sheet membrane configuration. The HF membrane preparation was done by dip coating, a frequently used process for the production of HF membranes, which involves the deposition of a thin film of a coating solution. Different thicknesses of the active layer were obtained by modifying the polymer content in the coating solution, allowing later to evaluate the influence of the thickness on the separation performance. This study includes a description of the procedure to prepare selective membranes, its characterization and an analysis of the influence of operating conditions on membrane separation performance. SEM and water contact angle were used to characterize the produced membranes. The mass transport phenomena in the pervaporation process were characterized using a resistances-in-series model. The results allow to adopt a criterion to select the most suitable thickness for the membrane active layer, which allows to achieve an adequate separation performance, and reveal the importance in the choice of the membrane support material. Finally, a comparative analysis of the self-made hollow fiber membranes performance in terms of flux, separation factor and PSI with respect to those found in the literature is presented.

## 1. Introduction

In recent years, policy makers, researchers and industry have taken more significant steps towards a bio-based economy. Problems related to the world's heavy dependence on fossil fuels such as volatility of the oil and energy production, the increasing crude oil prices, the pollution and the increasing emissions of greenhouse gases have set the search for renewable energy sources. Thus, biofuels such as butanol have become more attractive to fulfill the increasing fuel demand in the future. Second generation biofuels are now being produced from lignocellulosic biomass (such as perennial grasses), forestry materials, the co-products from food production, and domestic vegetable waste. n-Butanol is a very competitive biomass-based fuel that can be produced via ABE fermentation from renewable feedstocks (biobutanol). Given its advantages [1], it is a potential choice for renewable transportation fuel and considered a valuable commodity. It can be used as a solvent, in cosmetics, hydraulic fluids, detergent formulations, drugs, as a chemical intermediate in the

production of butyl acrylate and methacrylate, and as an extractant in the manufacture of pharmaceuticals [2–4]. On the other hand, the fermentative production process has some disadvantages over the petrochemical route (chemical synthesis) as the outcome of the process is very low in final butanol concentration (1–2 wt%) due to severe butanol toxicity to microorganisms, so that the process performance is low and cost intensive butanol recovery techniques are required [5]. Moreover, the high cost of production due to expensive pre-treatment technologies adds concerns on the economic feasibility [6].

Advances in production process such as the conversion process are necessary as they will improve the sustainability through better efficiencies and reduced environmental impact. In this frame, the large amounts of waste/residue biomasses from agro-food industries are a key resource to produce both bio-based products and second-generation fuels in order to improve the eco-sustainability of productions [2]. Further, the generation of biofuels may improve the local employment opportunities and contribute to the reduction of CO<sub>2</sub> emissions.

As mentioned above, the low concentration of ABE fermentation

\* Corresponding author.

E-mail address: [gorrie@unican.es](mailto:gorrie@unican.es) (D. Gorri).

<https://doi.org/10.1016/j.seppur.2021.119758>

Received 31 July 2021; Received in revised form 15 September 2021; Accepted 15 September 2021

Available online 20 September 2021

1383-5866/© 2021 The Author(s).

Published by Elsevier B.V. This is an open access article under the CC BY-NC-ND license

(<http://creativecommons.org/licenses/by-nc-nd/4.0/>).

| Nomenclature          |  |
|-----------------------|--|
| $a_i$                 | activity of component $i$ (mole fraction)  |
| $D_{\text{pore}}$     | Diameter of the pore (m)   |
| $F$                   | liquid flow rate ( $\text{L min}^{-1}$ )   |
| F-S                   | Flat sheet membrane  |
| HF                    | Hollow fiber membrane  |
| $J$                   | total flux ( $\text{kg m}^{-2} \text{s}^{-1}$ )  |
| $J_i$                 | flux of each component ( $\text{kg m}^{-2} \text{s}^{-1}$ )  |
| $J_{N, \text{total}}$ | thickness-normalized total flux ( $\mu\text{m kg m}^{-2} \text{s}^{-1}$ )                          |
| $k_{i, \text{bl}}$    | mass transfer coefficient for component ( $i$ ) at the liquid boundary layer ( $\text{m s}^{-1}$ ) |
| MW                    | molecular weight   |
| PDMS                  | poly(dimethyl siloxane)  |
| PEBA                  | poly(ether block amide)  |
| $P_i$                 | permeability of the membrane for component ( $i$ ) ( $\text{kmol s}^{-1} \text{m}^{-1}$ )          |
| POMS                  | polyoctylmethyl siloxane   |
| PP                    | poly(propylene)  |
| PSI                   | pervaporation separation index ( $\text{kg m}^{-2} \text{s}^{-1}$ )                                |
| PV                    | pervaporation  |
| $R_{i, \text{OV}}$    | overall mass transfer resistance ( $\text{s m}^2 \text{kmol}^{-1}$ )                               |
| $R_{i, \text{AL}}$    | mass transfer resistance in membrane active layer ( $\text{s m}^2 \text{kmol}^{-1}$ )              |
| $R_{i, \text{bl}}$    | liquid mass transfer resistance ( $\text{s m}^2 \text{kmol}^{-1}$ )                                |
| $R_{i, \text{M}}$     | membrane mass transfer resistance ( $\text{s m}^2 \text{kmol}^{-1}$ )                              |
| $R_{i, \text{Supp}}$  | mass transfer resistance in membrane support ( $\text{s m}^2 \text{kmol}^{-1}$ )                   |
| SEM                   | scanning electron microscope   |
| $u$                   | velocity ( $\text{m min}^{-1}$ )   |
| wt. %                 | composition expressed as percentage by mass  |
| $x_i$                 | mole fraction of component ( $i$ ) in the feed stream  |
| $y_i$                 | mole fraction of component ( $i$ ) in the permeate stream  |
| <b>Greek Letters</b>  |  |
| $\alpha_{i,j}$        | membrane selectivity (-)   |
| $\beta$               | separation factor (-)  |
| $\gamma_i$            | activity coefficient (-)   |
| $\delta$              | thickness of the membrane (m)  |
| $\rho_m$              | molar density of feed liquid ( $\text{kmol m}^{-3}$ )  |
| <b>Subscripts</b>     |  |
| AL                    | active layer   |
| SL                    | support layer  |
| bl                    | boundary layer   |
| F                     | feed   |
| i                     | component $i$  |
| m                     | membrane   |
| OV                    | overall  |
| P                     | permeate   |

products in the fermentation broth means that the cost of recovery and purification of these organic compounds is high, mainly due to the energy requirements in the applied separation processes. Conventional processes usually use a sequence of distillation operations. Due to the non-ideal behavior of the mixture to be separated, two of the organic compounds (ethanol and n-butanol) form azeotropes with water, and furthermore the n-butanol/water system is partially miscible. These phenomena add complexity to separation by distillation, requiring additional columns and a decanter to separate a two-phase stream. As Liu et al. [7] remarked, energy use is dependent on the product purity requirements for end use, as well as the composition of product in fermentation broth. Thus, the energy required to recover / concentrate n-butanol up to a purity of 99.5 wt% is in the range of 31–69.5 MJ kg<sup>-1</sup> [8,9]. This has been a motivation to study alternative separation processes, including gas-stripping, liquid-liquid extraction, and membrane technologies such as pervaporation and membrane distillation [5,10,11]. However, the need to obtain products with high purity motivates the convenience of using distillation, so that the best alternative seems to be a hybrid process that combines distillation with another non-conventional separation process, such as pervaporation, reducing the overall consumption of energy [9,12].

Lately, membrane-based separation technologies for the recovery of biofuels have motivated researchers compared to the conventional purification methods such as distillation. They may offer more capital and energy efficiency, small footprint, simplicity in operation, ease of scale up, and environmental friendliness. Pervaporation is considered one of the most promising membrane techniques to be integrated with fermentation for butanol separation. Presently, membrane pervaporation has shown potential for butanol separation [13,14] but, however, the efficiency of the process is still limited by the membrane performance. Indisputably, membrane fabrication has come a long way since the advent of asymmetric membranes by the Loeb and Sourirajan, considered a leading breakthrough, to obtain membranes with more mechanical stability, high throughput (flux) and efficiency (selectivity) [15].

Membrane modules with hollow fiber configuration present a series of characteristics that make them interesting for an application on an industrial scale, among which it can be highlighted that compact

modules with high membrane surface areas can be formed. Although hollow fiber membranes have been studied in various separation processes, their main application has been in gas permeation. The recent development of polymeric membranes focused on the combination of different polymers to produce composite membranes [16].

For a membrane to be used in pervaporation, the membrane is required to include a dense selective layer. In the case of hollow fiber membranes, the dense selective layer can be formed during fiber manufacture by a phase inversion process or, alternatively, by depositing a selective polymeric material on a porous support, such as in the process known as dip-coating, which has been used in this study to prepare composite membranes. The porous hollow fiber substrate offers the mechanical strength for the entire composite membrane, while the ultra-thin selective layer achieves the separation [17]. With regard to porous support, inorganic substrates exhibit the advantages of the chemical, mechanical and thermal stabilities. However, the use of polymeric materials is more desirable for industrial scale because they are easy to fabricate and provide good performance at low cost.

Different hydrophobic-organophilic polymeric membranes have been tested for the recovery of n-butanol by PV, as has been recently reported in some reviews [18–20]. Poly(dimethyl siloxane), often referred to as “silicone rubber,” is the most widely studied membrane material for bio-alcohol recovery. The studies reported in the literature on the application of PDMS membranes for the selective separation of biofuels have been recently reviewed by Wang et al. [21]. This study indicates that most of the reported studies used PDMS flat sheet membranes. However, several studies on the use of PDMS hollow fiber membranes for the selective removal of volatile organochlorine compounds have been reported [22,23]. Other materials tested for the selective separation of bio-alcohols include polyether block amide (PEBA), poly[1-(trimethylsilyl)-1-propyne] (PTMSP), polyurethane and composite membranes formed with a polymer matrix with the addition of fillers. Among these polymeric materials, PEBA is attracting the interest of researchers due to its affinity for n-butanol and its hydrophobic character that limits the solubility of water into the membrane. Several papers have reported the use of PEBA-based PV membranes for the selective separation of organic compounds from the ABE mixture since the

pioneering works by Boddeker et al. [24]. However, there are few previous works using PEBA-based membranes with hollow fiber configuration. Feng and col. have reported the preparation of hollow fiber membranes with a dense selective layer of PEBA by dip-coating and their application to the separation of various gas mixtures [25,26]. The main novelty of this work resides in the reporting of a study on the manufacture of HF membranes with an active dense layer of PEBAX-2533 using a commercial polymeric support, analyzing and discussing the preparation conditions of the membranes and their influence on the pervaporation separation performance. Although there are a good number of papers on the preparation and use of PEBA-based pervaporation membranes, many of them for butanol separation, the majority of cases correspond to flat sheet membranes. Among the few exceptions that correspond to studies made with tubular membranes based on PEBA, were membranes prepared on ceramic supports. Li et al. [27] reported an interesting work where PEBA/ceramic hollow fiber composite membranes with high flux were prepared by dip-coating the ceramic hollow fiber with PEBA polymer solution. The membrane fabrication was optimized by tailoring the coating parameters, such as the viscosity and concentration of PEBA coating solution, allowing to achieve permeation fluxes of up to  $4.2 \text{ kg m}^{-2}\text{h}^{-1}$ , with a selectivity of 21 when working with 1 wt% n-butanol-water mixtures at  $60^\circ\text{C}$ .

In this way, this work focuses on the development of polymeric hollow fiber membranes for the separation of butanol-ethanol-acetone aqueous solutions by PV. A methodology for the manufacture of HF membranes with a PEBA dense selective layer using the technique of dip coating by evaporation of the solvent is used. The most suitable conditions for manufacturing HF membranes using a commercial polymeric porous support are clearly established by linking them to separation performance. Laboratory techniques such as SEM and contact angle were used to characterize the produced membranes. Then, the characterization of the mass transfer through the membrane is presented. The influence of the active layer thickness of the membranes in the separation of ABE mixtures is also studied. Finally, a comparison of the HF membranes' performance with literature is discussed. Therefore, this study may provide useful insights into materials design and fabrication of composite hollow fibers for the separation of ABE mixtures from fermentation process by PV.

## 2. Experimental methodology

### 2.1. Materials

For the preparation of the coating solution the polymer PEBAX 2533 (CAS No. 77402-38-1) was kindly supplied by ARKEMA, France.

The aqueous feed solution for the PV experiments was prepared by mixing: 1-butanol (CAS No. 71-36-3), ethanol (CAS No.64-17-5) and acetone (CAS No. 67-64-1) with ultrapure water Milli Q obtained from a Merck-Millipore system (supplied by Merck KGaA, Darmstadt, Germany). All of the materials were of analytical grade and were used without further purification.

Polypropylene (PP) commercial hollow fibers membranes Celgard X-20 (supplied by Hoechst Celanese, Charlotte, NC, U.S.A.) were used as the support (Table 1).

**Table 1**  
Characteristics of the HF support structure.

| Membrane                            | Celgard X-20  |
|-------------------------------------|---------------|
| Material                            | polypropylene |
| Inner diameter ( $\mu\text{m}$ )    | 400           |
| Wall thickness ( $\mu\text{m}$ )    | 30            |
| $D_{\text{pore}}$ ( $\mu\text{m}$ ) | 0.115         |
| Fiber porosity (%)                  | 40            |

### 2.2. Dip coating

The coating solution used was prepared at different concentrations (0.25–12 %w/w) of PEBAX in 1-butanol. The polymer was dissolved using a heating plate at  $70^\circ\text{C}$  for 24 h with a propeller stirrer. Then it was left to rest for natural degasification and cooling for 24hrs. The final viscosity was measured using a rotational viscometer at room temperature.

The fabrication of ultrathin skin layer hollow fiber membranes still remains very difficult as indicated by Chung and col. [28]. To make an ultrathin selective-layer is the main challenge and thus different spinning dope formulations consisting on solvent/non-solvent or multi-solvents have been reported in literature. Here, the dip coating procedure consisted on immersing the commercial fibers in the coating solution (or dope solution) for few seconds to allow a thin film formation on the outer phase of the fibers. Covering of the ends of the fibers was previously done to prevent the dip coating solution from entering the fibers lumen. When a fiber is drawn out of a pure liquid bath, a meniscus is formed. Because of viscous forces and inertia effects fluid entrainment occurs on the fiber, whereby gravity and surface forces counteract. Since the fibers made are small fibers, at moderate coating velocities the gravity and inertial forces can be neglected. So the formation of a liquid film is described as a balance between viscous forces and surface tension as stated by Jesswein et al. [29].

After the dip coating was performed, the fibers were left to stand for 1–2 days at room temperature for the volatile solvent to be eliminated, resulting in a thin film of coating. After drying, the film hardened and then the dried dip coated hollow fiber membranes were placed inside a PV module, see Fig. 1. Finally, the module is filled up with epoxy resin to seal each end to prevent any leaks. The custom-made module contained 15 fibers with a length of 15 cm, and the total membrane area was  $28.3 \text{ cm}^2$  based on the internal diameter of the HF.

### 2.3. Membrane characterization

For the morphological characterization (microstructure and distribution of the polymer) of the membranes a scanning electron microscopy (SEM), model Zeiss EVO MA15 (Zeiss, Oberkochen, Germany) was used. Liquid nitrogen was used to freeze the membrane samples before performing the cut of the transversal cross-section area. This was done to prevent polymer deformation and to obtain an accurate measurement of the thickness of the dense selective layer of the membrane.

In order to evaluate hydrophobicity/hydrophilicity and wetting behavior of PEBA membranes, the static contact angles between the membrane and different chemical compounds were measured by the sessile liquid drop method using contact angle measurement system (DSA25, Krüss, Germany). For the goniometric measurements, flat sheet membranes were prepared separately by phase inversion dissolving 0.20 g of PEBAX in 5 mL of butanol to obtain a dense membrane with a thickness of about  $20 \mu\text{m}$ . They were deposited on a Petri dish and left over night to dry. Then they were cut and laid over on glass slides carefully, preventing any overstretching of the membrane. Then the slides were set on the apparatus with the holding system. The static contact angles were measured at room temperature. Adjusting of the picolitre dispenser (0.5 mm syringe) and camera image was also done before each component measurement. Then, a  $2.0 \mu\text{L}$  drop with the desired component was deposited on the membrane's surface at five different sites. Each value was obtained using the software provided through image recognition. The average contact angles value was then considered.

### 2.4. PV experiments

The PV performance was evaluated by a custom-built lab scale PV unit as described in a previous work [13]. A hollow fiber module was set up in the PV unit. Fig. 1 describes the module used in the PV unit as well

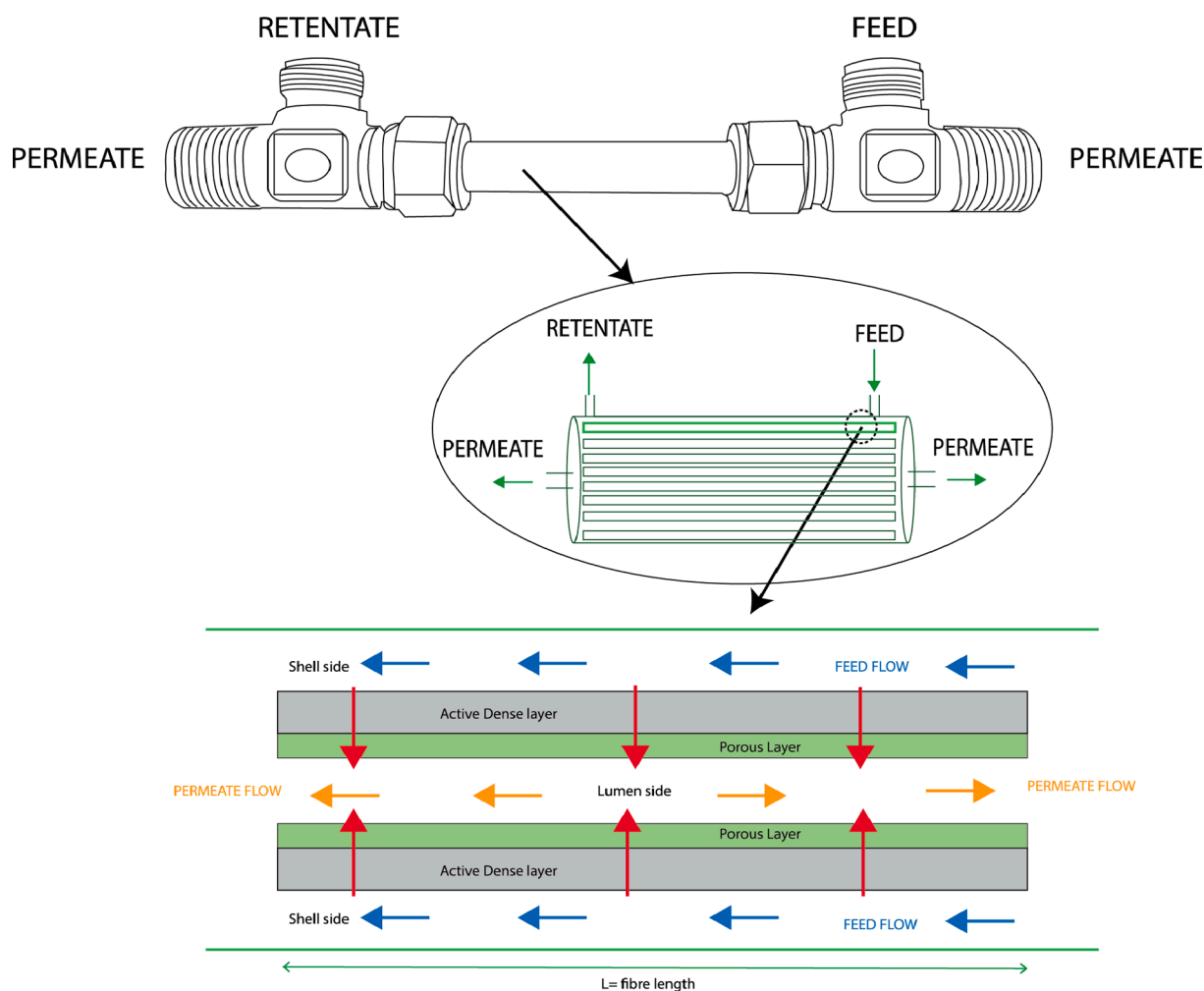


Fig. 1. HF membrane pervaporation module.

as the separation concept within the HF membrane. The separation process consists on the feed mixture passing through the shell side and when vacuum is applied the permeate comes out of the lumen side. According to the technical literature, the optimal temperature for the ABE fermentation is between 30 and 40 °C [30]. Taking into account that the membranes developed in this work could be used as a tool for the in situ removal of butanol from fermentation broths, a temperature of 40 °C was adopted to carry out the pervaporation experiments. All PV experiments were carried out flowing (1:2:1 wt%) ABE solutions, and the permeate side was maintained below 15 mbar using a diaphragm vacuum pump (Vacuubrand PC 3004 VARIO). Every 30 min samples of the feed and permeate were collected, weighed and analyzed in a gas chromatograph equipped with a flame ionization detector (GC-FID) model GC- 2010 from Shimadzu. Each PV experiment lasted for at least 4 h after the stabilization process, to be sure that a pseudo steady state was reached.

The PV performance of a membrane was evaluated in terms of permeate flux  $J$ , separation factor  $\beta$  and pervaporation separation index (PSI). Moreover the mass transfer in the system was also characterized using the resistances-in-series approach [31,32].

The total flux  $J$  ( $\text{kg m}^{-2} \text{h}^{-1}$ ) across the membrane is obtained relating the mass of permeate collected with the time interval and the membrane area. After that, the flux for each component  $J_i$  is calculated from the total flux and the permeate composition obtained by chromatographic analysis

As Lipnizki et al. [33] highlighted, relating the mass transport in pervaporation to only the mass transport through the membrane leads

generally to an overestimation of the efficiency of pervaporation. The pervaporation process is also influenced by the concentration boundary layer on the feed side, the support structure (as in our case, working with composite membranes) and the concentration boundary layer on the permeate side. These additional factors have to be taken into account to evaluate the membrane performance. Among the different resistances influencing the mass transport in pervaporation, the concentration boundary layer on the feed side is one of the key resistances in the overall process and can even dominate the separation process [33,34].

In the literature it is possible to find different expressions for the permeation flux through a membrane, depending on the approach chosen to express the driving force for mass transfer. Although from a thermodynamic point of view the driving force should be the chemical potential gradient of the species that permeate, other expressions are common in the pervaporation literature according to the simplifying hypotheses assumed in each case. In this work, an expression is adopted where the permeation flow is driven by an activity gradient. Thus, taking into account the possible contribution of different resistances, we adopt a flux equation that includes an overall mass transfer resistance from the bulk of the feed to the permeate side:

$$J_i = \frac{1}{R_{i,OV}} (a_{i,F} - a_{i,P}) \quad (1)$$

We will assume that the mass transfer rate is dominated by the mass transfer through the concentration boundary layer on the feed side and through the membrane. In turn, we are going to consider that the resistance of the membrane is due to the contributions of both the dense

active layer and the support, as it will later be proved. Thereby, adopting a resistances-in-series model, the overall mass transfer resistance for a component  $i$  can be described by:

$$R_{i,OV} = R_{i,bl} + R_{i,M} = R_{i,bl} + (R_{i,AL} + R_{i,Supp}) \quad (2)$$

$$R_{i,OV} = \left( \frac{\gamma_{i,F}}{k_{i,bl}\rho_m} \right) + \left( \frac{\delta}{P_i} + R_{i,Supp} \right) \quad (3)$$

Replacing Eq. (3) in Eq. (1) we obtain the expression for the permeation flux of component  $i$ :

$$J_i = \frac{(a_{i,F} - a_{i,P})}{\left( \frac{\gamma_{i,F}}{k_{i,bl}\rho_m} \right) + \left( \frac{\delta}{P_i} + R_{i,Supp} \right)} \quad (4)$$

In this work, a series of composite membranes with different thicknesses of the PEBAX active layer were prepared and the respective membrane modules were constructed, carrying out series of pervaporation experiments at different feed flow rates with each membrane module, so to obtain sufficient experimental data to allow evaluating the contribution of each of the mass transfer resistances.

The separation factor  $\beta_{i/j}$  is calculated as the ratio between the molar concentrations of the components in the permeate ( $y_{i/j}$ ) and the feed ( $x_{i/j}$ ) (Eq. (5)):

$$\beta_{i,j} = \frac{y_i/y_j}{x_i/x_j} \quad (5)$$

The membrane selectivity toward butanol ( $\alpha_{i/j}$ ) and the pervaporation separation index (PSI) are defined according to Eq. (6) and Eq. (7):

$$\alpha_{i,j} = \frac{P_i}{P_j} \quad (6)$$

where  $P_i$  is the permeability of butanol and  $P_j$  is the permeability of water

$$PSI = J \cdot (\beta_{i,j} - 1) \quad (7)$$

### 3. Results and discussion

#### 3.1. Membrane morphology

Morphological features of different composition HF membranes were analyzed by Scanning electron microscopy (SEM). Fig. 2 shows a SEM analysis of the external surface of a HF membrane surrounding the commercial polypropylene support. Pores are seen before depositing the polymer active layer by dip coating (Fig. 2a). Obtaining polymeric hollow fiber membranes with an ultrathin and defect-free selective layer is quite challenging. Thus, Fig. 2b shows how small pin hole defects appear on the surface of a membrane with a very thin dense layer < 1  $\mu\text{m}$ , similar to what it was found by Firpo et al. [35]. Finally, Fig. 2c

shows a homogeneous dense layer with no pores or defects after the coating. Fig. 3 shows SEM analysis of various HF membranes made with PEBAX solutions of different concentrations, resulting in active layer with distinct thicknesses (1  $\mu\text{m}$  – 61  $\mu\text{m}$ ). The figure shows how the thickness of the active layer becomes thinner across the images being (a) the thickest active layer and (h) the thinnest one. It can be stated that the active layer has a dense non-porous structure that is clearly distinguishable from the support. In the case of the support, conventional pores are not appreciated, which is explained by the fact that polypropylene fibers are manufactured by stretching.

#### 3.2. Contact angle

Hydrophilic / hydrophobic characteristic of the prepared membranes was evaluated by means of the contact angle. If a water drop is placed on a hydrophilic surface, it spreads as far as possible. Hydrophilic surfaces show low water contact angle (<90°) and hydrophobic surfaces show high water contact angle values (>90°) [36].

As observed in Table 2, the components of the mixture deposited on the prepared membrane all showed different measured contact angle values. The contact angles were always < 90° and the value decreased in the order of water/ethanol/butanol/acetone. The ABE mixture value is very close to the water value. Thus, the behavior of the membrane surface suggests, as expected, more affinity towards acetone and butanol and rejection to water. This could also reflect the polarity of the molecules, being water the most polar component with a contact angle of 76.8°, which it is in good agreement with the value of 78.8° that was reported by Gazic et al. [37] for PEBA membranes. Also, it shows that the surface of PEBA membranes is not highly hydrophobic, therefore the membranes would show better antifouling performance in fermentation broth [38]. Also included in Table 2 are the surface tension values for pure compounds (from Dortmund Data Bank), showing that the contact angle is influenced by the surface tension but does not depend solely on it but on the affinity between the components of the solution and the surface of the polymeric material.

Wetting is favored when the solid polymer has a high surface energy. As a reference, recently Selim et al. [39] have reported a value of 80° for the water contact angle with PEBAX 2533 pristine membranes and have calculated the surface free energy (SFE) for the polymer, finding that the dispersive contribution to SFE was 32  $\text{mN m}^{-1}$  and the polar contribution it was 2.5  $\text{mN m}^{-1}$ , which is consistent with the hydrophobic character of the polymer.

Numerous studies have shown the utility of using Hansen solubility parameters (HSPs) to provide a measure of the mutual affinity of the permeating compounds and the membrane [40]. Solubility parameter theory is an approach to predict polymer-liquid interactions with the help of the polymer structure and polarity of the liquids that need to be separated. For the specific case of the interaction between the PEBAX 2533 polymer and the components of the ABE mixture, the HSP values

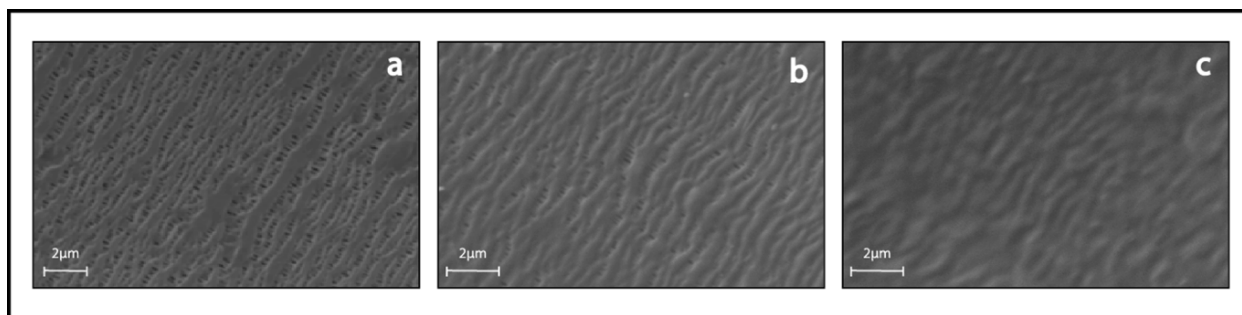
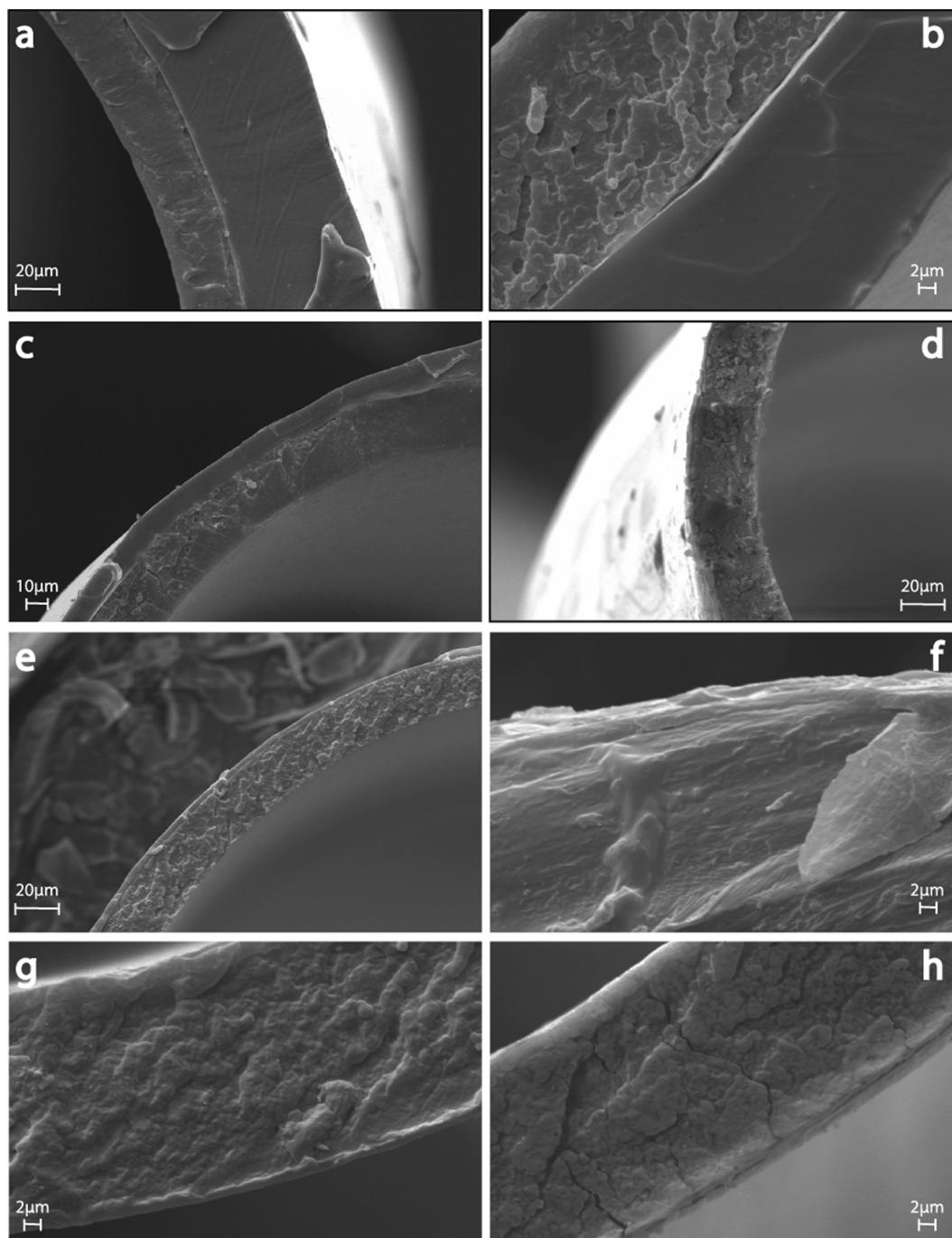


Fig. 2. SEM analysis of the surface of the HF membrane: a) Support of polypropylene; b) Membrane with a very thin active layer of PEBAX showing defects; c) Membrane with a free-defect active layer of PEBAX.



**Fig. 3.** SEM analysis of the cross section of the HF modified membranes with different polymer concentration: (a) 12% (61  $\mu\text{m}$ ), (b) 11% (24  $\mu\text{m}$ ), (c) 8.3% (10.2  $\mu\text{m}$ ), (d) 7.5% (3  $\mu\text{m}$ ), (e) 5% (2.8  $\mu\text{m}$ ), (f) 2.5% (1.8  $\mu\text{m}$ ), (g) 1% (1  $\mu\text{m}$ ), (h) 0.5% (1.1  $\mu\text{m}$ ).

**Table 2**

Contact angle measured for PEBAX and ABE components.

| Liquid      | Measured contact angle [°] | Surface tension ( $\text{mN m}^{-1}$ ), 293.15 K |
|-------------|----------------------------|--|
| Butanol     | 38.4                       | 24.6   |
| Ethanol     | 55.0                       | 22.3   |
| Acetone     | 32.4                       | 23.3   |
| Water       | 76.8                       | 72.8   |
| ABE mixture | 70.2                       |  |

have been reported by Heitmann et al. [41]. According to the values reported in that study, PEBA 2533 would have the highest affinity towards acetone, followed by butanol, ethanol and little affinity towards

water. This order coincides with that of the contact angles measured in this work. However, experimental studies have reported that the sorption of n-butanol was found to be the highest, followed by acetone and ethanol [41,42]. Liu and Feng [42] reported sorption experiments on PEBAX 2533 at 23 °C, which showed that the solvent uptake in the polymer (in g solvent/g polymer) is 6.83, 0.71 and 0.56 for n-butanol, acetone and ethanol, respectively. The higher solubility of n-butanol in PEBAX with respect to ethanol and acetone was later confirmed in the work by Heitmann et al. [41]. Similar findings regarding the discrepancies in the order of solvent uptake observed experimentally for components of ABE mixture and the order predicted by the analysis of the HSPs was reported by Niemistö et al. [43] for PDMS membranes. Thus,

as Heitmann et al. [41] remarked, Hansen solubility parameters can be used to roughly predict whether a solvent is likely to dissolve in a polymer material or not, however, a detailed prediction of the sorption behavior is not possible. Jirsáková et al. [44] have attributed the discrepancies in the predictions with HSPs for solvent uptake in PEBAX 2533 to the very different nature of the hard PA block and the soft PE block in this polymer that does not allow to use a single solubility parameter for the whole sample.

The following Fig. 4 shows the drop shape of different substances at the time of measuring the static contact angle on the surface of a flat sheet PEBA membrane having a more spherical shape for water and flatter shapes for the rest of the components. The images relate to the very first moment when the drop of the component comes into contact with the PEBA surface.

In general, the shape of the water remained very steady during the whole measurement. The contact angle was recorded several times at the moment of the contact between the drop and the membrane. The measurement for water was very straightforward as no much variation was seen on the drop size, shape or volume. On the other hand, the solvents contact angle measurements experienced more variation as time went by making it a bit more difficult for the software to stabilize a correct reading measurement. This could be due to some external factors that influence its wettability character over the PEBA membrane such as evaporation, extension of the drop and absorption by the membrane. For butanol, a thicker membrane (34  $\mu\text{m}$ ) was used for the measurement to compensate for the swelling effect of the pure alcohol. Nevertheless, the data obtained hints on the affinity character of the membrane towards butanol. Finally, as seen, the hydrophobicity/wettability character of the membrane could highly contribute to the efficient removal of the solvents from water during the pervaporation of the ABE process.

The contact angle values between pure butanol and PEBA membranes measured in this work differ from others previously reported in the literature. Thus, contact angles of  $5^\circ$  and  $17.7^\circ$  were reported by Li et al. [27] and Liu et al. [38], respectively. According to Li et al. [45] some fluids such as nematic liquid crystals, water–oil–surfactant systems, ionic liquids, and dilute aqueous long-chain alcohols have an anomalous surface tensions that increase with temperature when the temperature exceeds a certain value, which are termed as “self-

rewetting fluids” [46]. Thus, more studies should be considered for the contact angle shift since there might be several phenomena affecting the process such as the Marangoni effect for self-rewetting fluids, due to concentration gradient and the thermocapillary flow [46,47]. Also, Talik et al. [48] studied the interfacial hydrogen interactions on the behavior of confined substances to evaluate the impact of the dynamics of alcohols having tendencies to form supramolecular structures of different architecture. This means that a change in chemical structure and architecture of supramolecular structures might be related to the surface effects between alcohols and porous material, a peculiar behavior of the self-assemblies at the interface [49]. Therefore, measuring the contact angle of alcohols is not a trivial procedure, those quantities also depend on microchannel geometry, surface roughness and local fluid conditions [50].

Drop interaction with solid surfaces upon impact has also interested researchers lately. Antonini et al. [51] studied the rebound of a drop from a surface when the wettability is low, i.e., when contact angles, measured at the triple line (solid–liquid–air), are high. However, no clear criterion exists to predict when a drop will rebound from a surface and which is the key wetting parameter to govern drop rebound. Also, Guo et al. [52] explain how surface wettability, viscosity and surface tension of fuels such as butanol have significant effects on spreading and rebounding behavior of the droplets. It was found that the receding contact angle is the key wetting parameter that affects rebound of droplets, along with surface hydrophobicity. However, the combined effect of wettability and wall temperature on the rate of different fuels evaporation is still unclear. But, the difference in rebounding degree is mainly determined by the resultant of inertial force of the droplet, adhesive force between the droplet and the surface and also counterforce of the solid wall. This rebound effect during the measurement of the contact angle of the ethanol, butanol and acetone was also appreciated.

### 3.3. Viscosity and layer thickness

Different hollow fiber membranes were prepared by dip coating using different concentrations (wt.%) of the coating solution (PEBAX/butanol): 0.25 %, 0.5 %, 1 %, 2 %, 2.5 %, 5 %, 7.5 %, 7.8 %, 10 %, 11 % and 12 %. It was found that the viscosity of the mixture during the dip

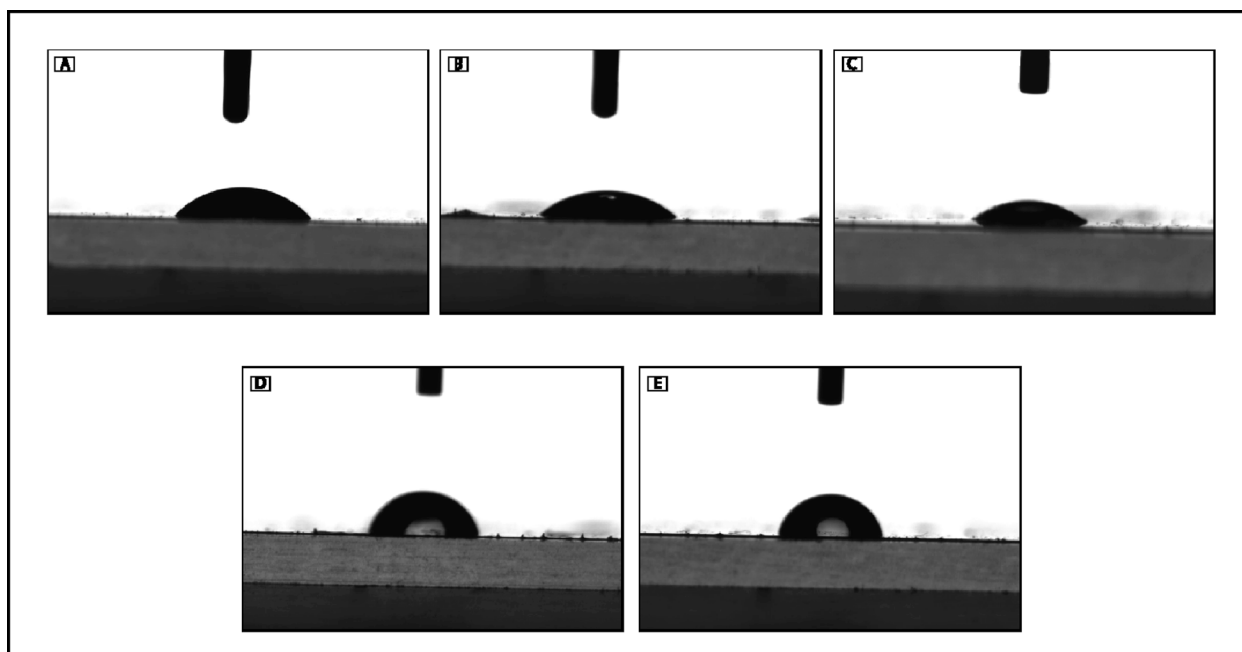
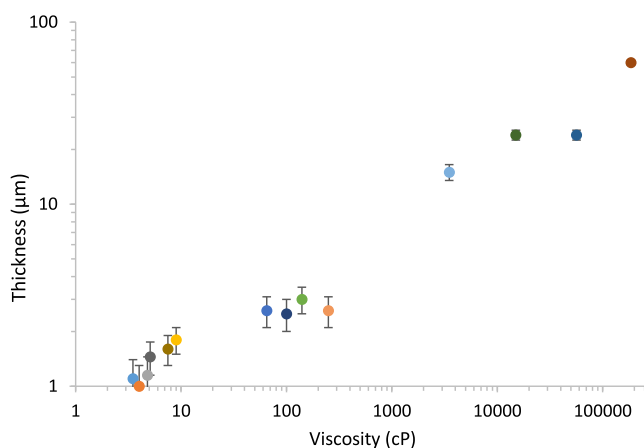


Fig. 4. Drop shape of: (a) butanol, (b) ethanol, (c) acetone, (d) water, (e) ABE solution when measuring the static contact angle on the active layer surface.

**Table 3**

Thickness of the active layer for different polymer content in the coating solution.

| % PEBAX | Viscosity (cP) | Thickness ( $\mu\text{m}$ ) |
|---------|----------------|-----------------------------|
| 0.25    | 3.5            | 1.1                         |
| 0.5     | 4              | 1.0                         |
| 1       | 4.8            | 1.15                        |
| 1       | 5.1            | 1.45                        |
| 2       | 7.5            | 1.6                         |
| 2.5     | 9              | 1.8                         |
| 5       | 65             | 2.6                         |
| 7.5     | 140            | 3.0                         |
| 7.8     | 100            | 2.5                         |
| 8.4     | 250            | 2.6                         |
| 8.9     | 3500           | 15                          |
| 10      | 56,500         | 24                          |
| 11      | 15,000         | 24                          |
| 12      | 185,000        | 60                          |



**Fig. 5.** Influence of viscosity of the coating solution on the thickness of the membrane dense (active) layer.

coating procedure influenced the thickness of the active layer. Table 3 shows how the thickness of the active layer ranged from 1 to 60  $\mu\text{m}$  as the concentration of the PEBAX coating solution and the viscosity increased.

Fig. 5 shows an indicative relationship about how the thickness of the dense PEBAX layer obtained by dip-coating depends on the viscosity of the coating solution at room temperature. This trend is indicative, especially due to the practical difficulty in handling polymer solutions with high viscosity and non-Newtonian behavior [53]. However, it is remarkable that Fig. 5 provides us with a useful guide to choose the characteristics of the coating solution when it is intended to obtain dense layers with a thickness  $<5 \mu\text{m}$ .

### 3.4. Mass transfer resistances in hollow fiber pervaporation

Modified HF membranes were fabricated with different active layer thicknesses in order to evaluate the importance of individual mass transfer resistances. PV experiments were performed with each membrane module flowing (1:2:1 wt%) ABE solutions at 40 °C and different flow rates (0.2, 0.3, 0.5, 1.2, 2.0 and 4.5  $\text{L min}^{-1}$ ). For each experiment, the partial permeation fluxes were related to the driving force (activity gradient) to obtain the overall resistance to mass transfer (see Eq. (1)). The activity coefficients for the components in the liquid feed mix were evaluated by the NRTL method using the Aspen Plus software. Then, a sequential procedure was followed to discriminate the contributions of the mass transfer resistance in the liquid boundary layer and in the membrane (active layer and support), assuming negligible resistance in

the vapor phase.

First, the total resistance was fitted (Wilson plot) by the reciprocal of the lineal velocity  $u$  ( $\text{m min}^{-1}$ ) through the membrane module raised to an exponent of 0.9, factor used for parallel flow in membrane contactors [54,55]. Then, the membrane mass transfer resistance was obtained from the y-intercept and the liquid mass transfer resistance was calculated from the slope of the total resistance in the system. In Fig. 6 the overall resistance for each component for four modified HF membranes with different active layer thicknesses at different flow rates is shown. Since the membrane active layer and support resistances are not a function of the liquid velocity, the addition of these resistances corresponds to the y-intercept of this plot. It was seen that the higher the flow rate the higher the velocity and the overall resistance decreases. Moreover, as the thickness of membrane increases also the overall resistance increases. Since the graphs show no cut in the origin thus for a maximum flow rate, the membrane resistance is the one responsible for the overall total resistance and the liquid resistance would be almost negligible, as seen in Fig. 7, where the percentage contribution of the membrane and liquid resistance is shown. Thus, the smaller the thickness of the active layer, the less overall resistance. However, as the flow rate decreases, the liquid resistance becomes more important. The data showed the membrane resistance as the most influential factor. The liquid resistance highly depends on the flow rate of the PV experiment. It is small compared to the membrane resistance, and a good indicator in the case of concentration polarization.

The procedure described above, using the Wilson plot, has allowed us to obtain representative values of the global resistance of the membrane, which encompasses the contributions of the dense selective layer and the support. Using the information about the thicknesses of the active layer obtained by SEM analysis, next we will show the procedure carried out to differentiate both resistances. According to equation (8), representing the (overall) membrane resistance for each permeant as a function of the thickness of the active layer, the y-intercept corresponds to the resistance of the support and the reciprocal value of the slope represents the intrinsic permeability of the active layer for the permeating species.

$$R_{i,M} = \frac{\delta}{P_i} + R_{i,Supp} \quad (8)$$

As an example of the applied procedure, Fig. 8 shows the data for the case of butanol permeation. The results obtained for the four permeating species are shown in Table 4.

The results obtained show the importance of taking into account the contribution of the support to the overall mass transfer resistance, especially in composite membranes where a very thin active layer has been deposited. In the previous literature, it is possible to find several works that analyze the role of the membrane support. Among them, some works propose from a theoretical point of view that the mass transfer through the support takes place by a diffusional mechanism in the pores, assuming that the mass transfer rate is controlled by the Knudsen diffusion or by a combined mechanism including both Fickian and Knudsen diffusion, depending on the dimensions of the support pores and the pressure on the permeate side [56,57]. In our case, if the hypothesis of a resistance in the support controlled by Knudsen diffusion were true, this would imply that the support resistance for permeating species should be inversely proportional to the Knudsen diffusion coefficient, that is, inversely proportional to the molecular weight. However, as shown in Table 4, the highest resistance of the support corresponds to water and the lowest to butanol, which weakens the hypothesis that the controlling mechanism is diffusion in the support pores (polypropylene). On the other hand, it is also possible to find in recent literature a series of interesting contributions that shed light on this point, showing that a frequent situation in composite membranes for pervaporation corresponds to one where an intrusion of the coating material takes place into the support pores [58–60]. Although most previous studies refer to PDMS as coating material, a certain analogy can be established for the

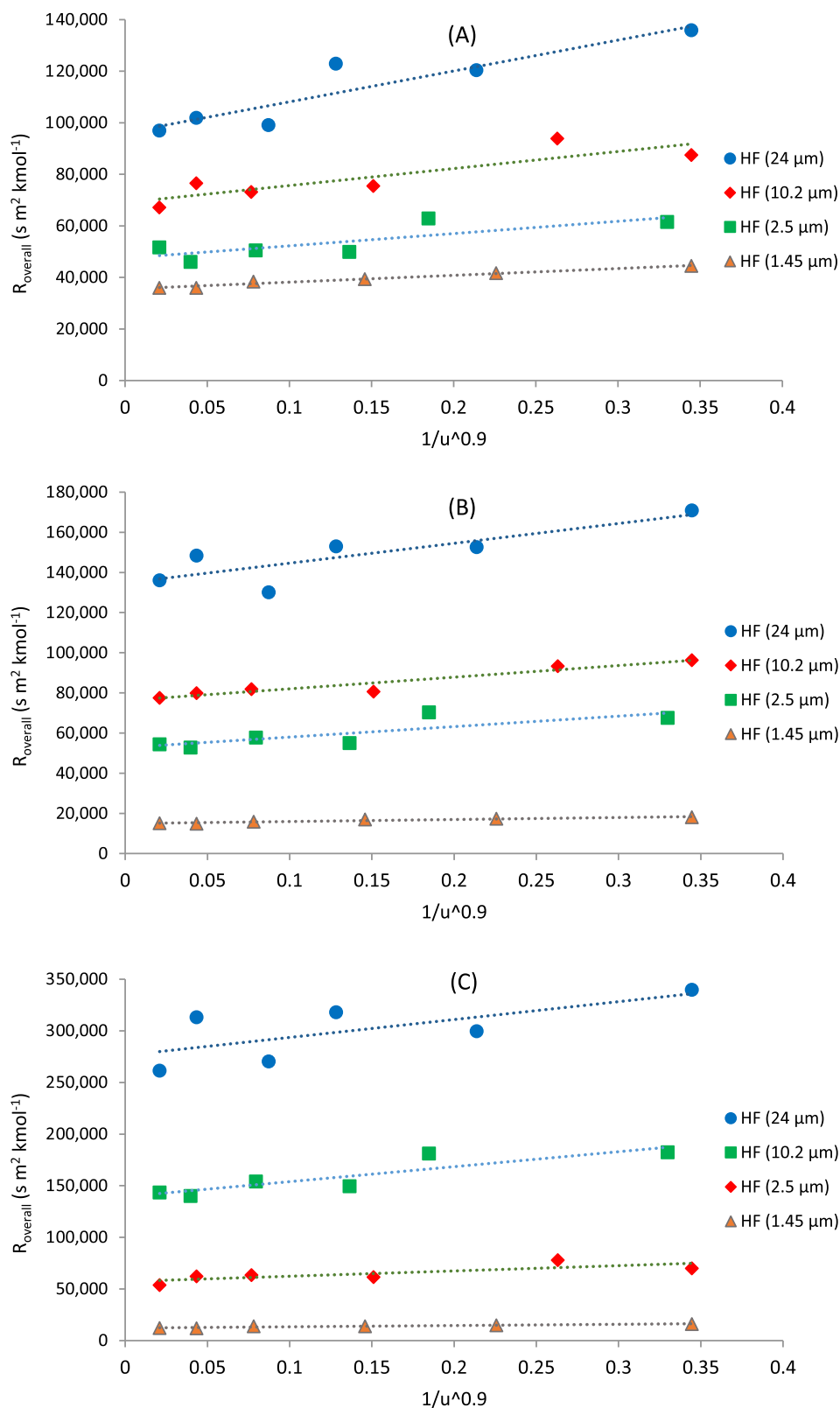


Fig. 6. Overall resistance of ABE components in a pervaporation process in a HF membrane contactor: (a) butanol, (b) ethanol, (c) acetone and (d) water.

case of PEBAX as coating material. Naik et al. [59] have pointed out that when the coating solution is highly viscous, a thick top layer is obtained, whereas pore intrusion and defects are obtained when not viscous enough. It is thus desirable to have a coating solution with a relatively

low polymer concentration to have the layer thin enough, but with adequate viscosity to prevent by intrusion and defect creation.

Although the hollow fiber membranes used for the experiments reported in Fig. 8 have been prepared with coating solutions of different

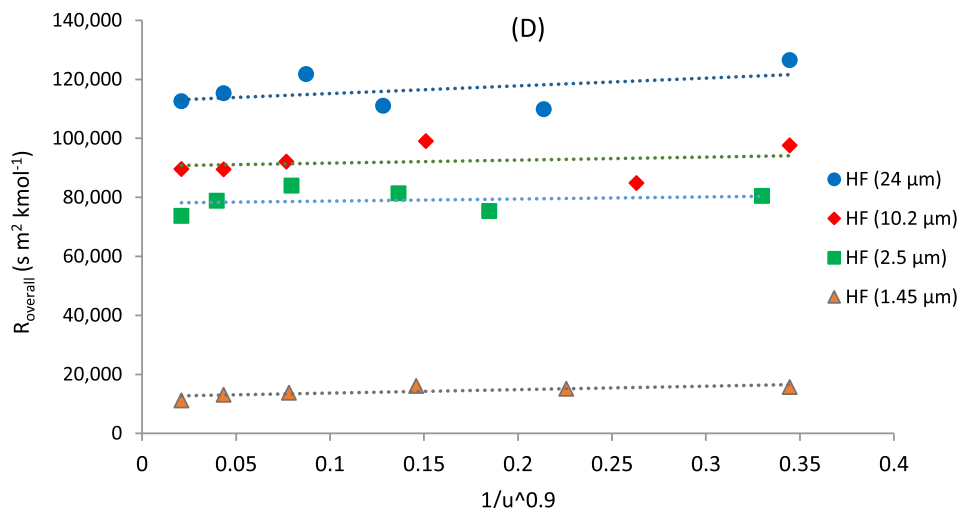


Fig. 6. (continued).

concentrations (and therefore with different viscosities), which could lead to different depth of intrusion into the support, it can be seen in Fig. 8 that the results corresponding to the membranes with active layer thicknesses higher than 2.5  $\mu\text{m}$  can be described assuming the same support resistance value ( $43.7 \times 10^3 \text{ m}^2 \text{ s kmol}^{-1}$  for butanol) for the tested membranes. On the other hand, the result obtained with the thinnest membrane (active layer thickness of 1.45  $\mu\text{m}$ ) is also included in Fig. 8, which clearly does not follow the trend due to defects in the active layer that explain the anomalous high flux and low selectivity values.

Analyzing the active layer permeability values for the organic compounds reported in Table 4, these follow the order butanol > ethanol > acetone, which is the same order found in a previous work [13] when PEBAX 2533 dense homogeneous (unsupported) membranes were used. The intrinsic selectivity of the membrane towards butanol is explained by the preferential sorption of butanol.

Regarding the mass transfer resistance of the support for the different permeating species (Table 4), these resistances are of a similar magnitude for organic compounds but it is clearly higher for water, which highlights the importance of choosing the appropriate material for the support layer. Thus, the support resistance has the contributions of the material that constitutes the active layer (PEBAX 2533) and the material that forms the support (polypropylene), which is a highly hydrophobic material. Although some interesting studies have undertaken the modeling of the effect of active layer intrusion inside the support pores [61,62], in our case it is difficult to determine the depth of the active layer intrusion into the pores, taking into account that the polypropylene support does not have a well-defined pore structure. The results obtained highlight the importance of choosing the material for the support because, instead of an ideal situation where the support only provides mechanical stability, its influence in the form of additional resistance can be very important.

### 3.5. Separation performance of the membranes

Once the discrimination of the mass transfer resistances that affect the permeation process through the HF membranes has been carried out, a comparison of the performance of different membranes prepared in this work has been made. For this, the data from the experiments carried out with the different membrane modules at a feed liquid flow rate of 4.5  $\text{L min}^{-1}$  have been used, as this is the operating condition with the lowest influence of concentration polarization. To carry out the comparison, the values of total permeation flux, separation factor and the pervaporation separation index (PSI) have been taken into account. In

Table 5 a summary of the experimental results obtained for HF membranes with active layer thicknesses in the range 1.45–24  $\mu\text{m}$  is shown. As already indicated above, the anomalous results obtained with the thinner membrane can be attributed to defects in the dense selective layer, leading to poor performance with high fluxes and low selectivities, being included here only as a reference. Regarding membranes that can be considered defect-free, it is interesting to note that, although a trade-off between permeation flux and separation factor is usually expected, here we can observe both flux and separation factor increased moderately as the active layer is thinner, as shown in Table 5. This tendency of the separation factor can be justified by the role of the membrane support (with PEBAX polymer intrusion into the pores), which provides additional resistance that affects water to a greater extent than organic compounds. Thus, as the active dense layer becomes thinner, both butanol flux and water flux increase, but proportionally the increase in butanol flux is greater, which can be seen in the permeate composition.

The membrane with a dense layer thickness of 2.5  $\mu\text{m}$  is the option with the best performance, with a permeation flux and separation factor of 1.33  $\text{kg m}^{-2} \text{ h}^{-1}$  and 21.2, respectively, when operating at 40  $^\circ\text{C}$  with a quaternary feed mixture with a composition similar to ABE solution (1:2:1 wt%). For this membrane the butanol content in the permeate was 28.1 wt%, clearly showing the potential to selectively recover it from aqueous solutions. Efforts made to obtain membranes with a dense layer thickness below 2  $\mu\text{m}$  resulted in membranes with micro-defects that showed lower separation performance.

Since the fiber length is usually around 1–1.5 m for industrial applications, we have performed a simulation to evaluate the influence of the active dense layer thickness and the feed flow rate on the separation performance for a hypothetical membrane module 1 m in length. Starting from the equations that describe the mass transfer in the HF membranes (Eqs. 1–8), a distributed parameter model was implemented in Aspen Custom Modeler and a series of simulations were run. As shown in Fig. 9a and 9b, the most favorable results in terms of PSI and butanol content (wt.%) in the permeate stream correspond to the hollow fibers with the thinnest thickness of the selective layer considered (2.5  $\mu\text{m}$ ) and the highest feed flow rate (4.5  $\text{L min}^{-1}$ ). Fig. 9a and 9b show, once again, the important effect of the feed flow rate on the separation performance. Thus, taking the case of the membrane with a selective layer thickness of 2.5  $\mu\text{m}$ , increasing the flow rate from 0.2 to 4.5  $\text{L min}^{-1}$  (which corresponds to a Reynolds number interval of 340–7700), the contribution of the boundary layer resistance to the overall mass transfer resistance decreases from 32 % to 2.8 % for butanol.

In order to compare the separation performance of the membranes

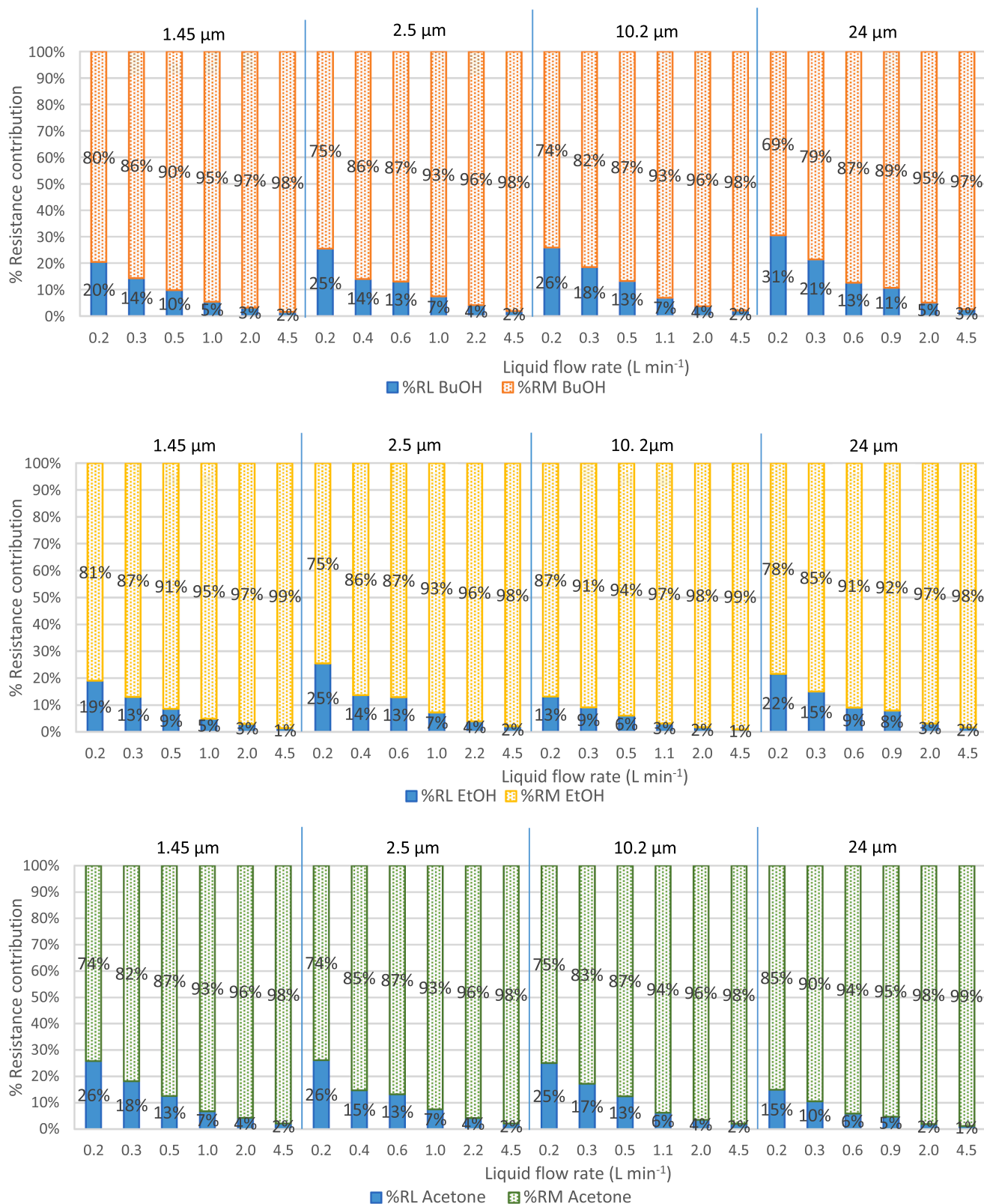


Fig. 7. Membrane and liquid resistance contribution on each membrane at different thickness of the active layer.

described in this work with other studies reported in the literature, Fig. 10 includes separation factor and permeation flux data, most of which were collected in the review paper by Kujawska et al. [19] to which the results corresponding to the HF membranes of this work and

the flat sheet (FS) membranes from our previous work [13] have been added.

Since there is usually a trade-off between membrane permeability and selectivity, the pervaporation separation index (PSI), which is

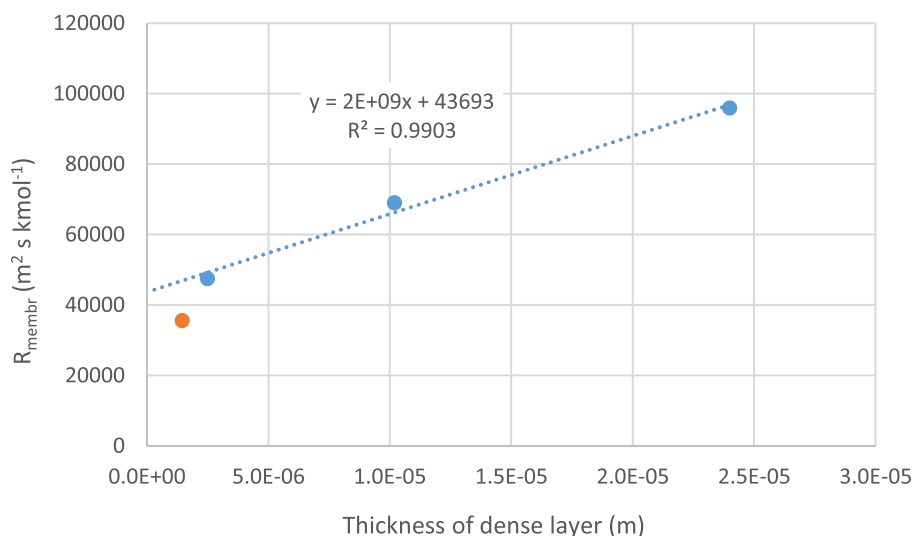


Fig. 8. Evaluation of the contributions of active layer and support to the (overall) membrane resistance for butanol permeation.

Table 4

Mass transfer resistance of the support and permeability of the membrane active layer.

| Compound | MW (kg kmol <sup>-1</sup> ) | Resistance in support (m <sup>2</sup> s kmol <sup>-1</sup> ) | Knudsen diffusivity (m <sup>2</sup> s <sup>-1</sup> ) | Permeability (kmol m <sup>-1</sup> s <sup>-1</sup> ) |
|----------|-----------------------------|--|---|--|
| butanol  | 74.12                       | 43.7 × 10 <sup>3</sup>                                       | 1.15 × 10 <sup>-5</sup>                               | 4.5 × 10 <sup>-10</sup>                              |
| ethanol  | 46.07                       | 42.4 × 10 <sup>3</sup>                                       | 1.45 × 10 <sup>-5</sup>                               | 2.7 × 10 <sup>-10</sup>                              |
| acetone  | 58.08                       | 31.5 × 10 <sup>3</sup>                                       | 1.30 × 10 <sup>-5</sup>                               | 9.5 × 10 <sup>-11</sup>                              |
| water    | 18.02                       | 74.7 × 10 <sup>3</sup>                                       | 2.33 × 10 <sup>-5</sup>                               | 6.7 × 10 <sup>-10</sup>                              |

Table 5

Comparative performance of HF membranes with different active layer thicknesses.

| Thickness (μm) | Butanol separation factor (β) | PSI (kg m <sup>-2</sup> h <sup>-1</sup> ) | J <sub>total</sub> (kg m <sup>-2</sup> h <sup>-1</sup> ) | J <sub>BuOH</sub> (kg m <sup>-2</sup> h <sup>-1</sup> ) | J <sub>EtOH</sub> (kg m <sup>-2</sup> h <sup>-1</sup> ) | J <sub>acetone</sub> (kg m <sup>-2</sup> h <sup>-1</sup> ) | J <sub>water</sub> (kg m <sup>-2</sup> h <sup>-1</sup> ) | J <sub>N<sub>2</sub>, total</sub> (μm kg m <sup>-2</sup> h <sup>-1</sup> ) |
|----------------|-------------------------------|---|--|---|---|--|--|--|
| 1.45           | 4.6                           | 24.5                                      | 6.79   | 0.52  | 0.19  | 0.33   | 5.75   | 9.85   |
| 2.5            | 21.2                          | 26.7                                      | 1.33   | 0.37  | 0.05  | 0.09   | 0.81   | 3.32   |
| 10.2           | 19.9                          | 21.1                                      | 1.12   | 0.29  | 0.04  | 0.03   | 0.77   | 11.4   |
| 24             | 17.4                          | 13.2                                      | 0.81   | 0.20  | 0.02  | 0.02   | 0.57   | 19.4   |

Operating conditions: 40 °C; liquid flow rate: 4.5 L min<sup>-1</sup>; feed mixture: (1:2:1 wt%) ABE solutions

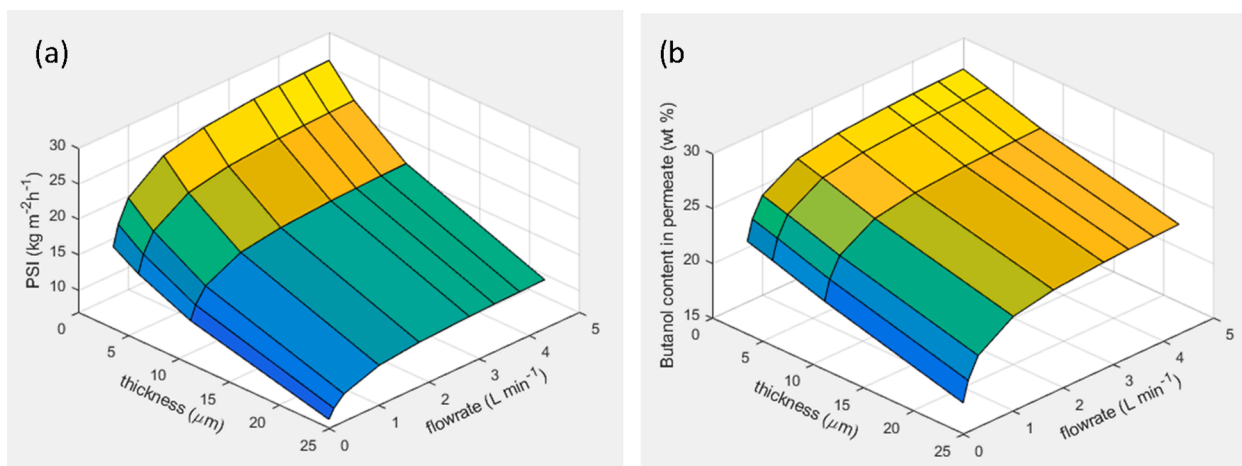


Fig. 9. Simulation showing the influence of the feed flow rate and thickness of the active dense layer on: a) PSI, and b) butanol content in permeate (wt.%), for a membrane module 1 m in length (Operating conditions: 40 °C; downstream pressure: 15 mbar; feed mixture: (1:2:1 wt%) ABE solutions).

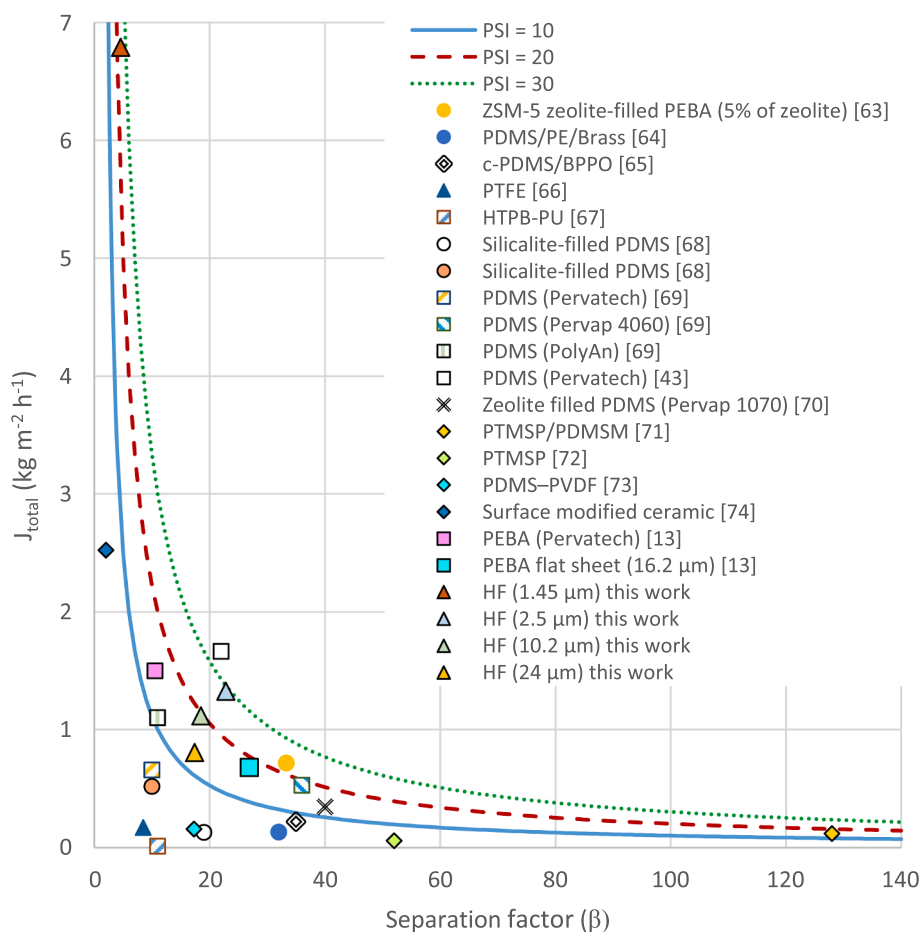


Fig. 10. Comparison of performance for different membranes with selectivity toward butanol. (Adapted from [19] with permission of Elsevier). (See above mentioned references for further information)

calculated according to Eq. (7), is commonly used to evaluate the overall performance of a membrane. Lines corresponding to constant values of PSI were used to compare the efficiency of various membranes in butanol recovery from aqueous solutions. It can be observed that most of the commercial (flat sheet) membranes, under similar conditions to our work, present PSI values between 10 and 20  $\text{kg m}^{-2}\text{h}^{-1}$ . Taking this into account, the membranes developed in this study and that present PSI values above 20  $\text{kg m}^{-2}\text{h}^{-1}$  are an interesting alternative because they would allow the construction of compact pervaporation membrane modules with high throughput.

#### 4. Conclusions

In this work, a procedure for the preparation of composite hollow fiber membranes with a dense selective layer of polyether-block-amide has been developed. The experimental results have revealed the importance of the coating solution viscosity as a guiding parameter regarding the thickness of the dense layer that can be obtained by the dip-coating procedure. Thus, the thickness of the coating increases with the viscosity of the coating solution, making it possible to obtain defect-free membranes with thicknesses as thin as 2.5  $\mu\text{m}$ . Although even thinner coatings, on the order of 1  $\mu\text{m}$ , were also obtained, their subsequent testing showed that these membranes had microdefects that affected the separation performance.

A study on the influence of operating conditions revealed that, under working conditions (40  $^{\circ}\text{C}$  and downstream pressure below 15 mbar) fluid dynamic conditions can significantly influence the separation achieved. Thus, the mass transfer resistances during separation are

mainly determined by the resistance in the liquid boundary layer and the resistance in the membrane itself, observing that at low feed flow rates the contribution of the resistance in liquid phase could reach up to 30% of the overall mass transfer resistance.

Regarding the mass transfer resistance of the support for the different permeating species (due to the intrusion of the coating material into the support pores), these resistances are of a similar magnitude for organic compounds but it is clearly higher for water, which highlights the importance of choosing the appropriate material for the support layer. Considering the active layer permeability values for the organic compounds, these follow the order butanol > ethanol > acetone, where the intrinsic selectivity of the membrane towards butanol is explained by the preferential sorption of butanol.

Finally, comparing these results with others previously reported in the literature, it is observed that the HF membranes developed in this study present PSI values similar or slightly higher than the commercial membranes with flat-sheet configuration currently available, therefore they constitute an interesting alternative because they would allow the construction of compact pervaporation membrane modules with high throughput.

#### CRedit authorship contribution statement

**Carla Arregoitia-Sarabia:** Conceptualization, Investigation, Writing – original draft. **Daniel González-Revuelta:** Investigation. **Marcos Fallanza:** Writing – review & editing, Methodology, Supervision. **Alfredo Ortiz:** Investigation, Funding acquisition. **Daniel Gorri:** : : Writing – review & editing, Supervision, Funding acquisition.

## Declaration of Competing Interest

The authors declare that they have no known competing financial interests or personal relationships that could have appeared to influence the work reported in this paper.

## Acknowledgements

This research is being supported by the Spanish AEI under the projects PID2019-104369RB-I00 and RTI2018-093310-B-I00, and by the Project ENERGY PUSH SOE3/P3/E0865, which is co-financed by the European Regional Development Fund (ERPF) in the framework of the INTERREG SUDOE Programme. Carla Arregoitia also thanks for a FPI research scholarship (BES-2017-081708).

## Appendix A. Supplementary material

Supplementary data to this article can be found online at <https://doi.org/10.1016/j.seppur.2021.119758>.

## References

- E. Sánchez-Ramírez, J.J. Quiroz-Ramírez, S. Hernández, J.G. Segovia-Hernández, A.A. Kiss, Optimal hybrid separations for intensified downstream processing of biobutanol, *Sep. Purif. Technol.* 185 (2017) 149–159, <https://doi.org/10.1016/j.seppur.2017.05.011>.
- V. García, J. Pääkkilä, H. Ojamo, E. Muurinen, R.L. Keiski, Challenges in biobutanol production: How to improve the efficiency? *Renew. Sustain. Energy Rev.* 15 (2011) 964–980, <https://doi.org/10.1016/j.rser.2010.11.008>.
- C. Jin, M. Yao, H. Liu, C.F. Lee, J. Ji, Progress in the production and application of n-butanol as a biofuel, *Renew. Sustain. Energy Rev.* 15 (2011) 4080–4106, <https://doi.org/10.1016/j.rser.2011.06.001>.
- S.Y. Lee, J.H. Park, S.H. Jang, L.K. Nielsen, J. Kim, K.S. Jung, Fermentative butanol production by clostridia, *Biotechnol. Bioeng.* 101 (2008) 209–228, <https://doi.org/10.1002/bit.22003>.
- N. Abdehagh, F.H. Tezel, J. Thibault, Separation techniques in butanol production: Challenges and developments, *Biomass and Bioenergy.* 60 (2014) 222–246, <https://doi.org/10.1016/j.biombioe.2013.10.003>.
- B.V. Ayodele, M.A. Alsaffar, S.I. Mustapa, An overview of integration opportunities for sustainable bioethanol production from first- and second-generation sugar-based feedstocks, *J. Clean. Prod.* 245 (2020), 118857, <https://doi.org/10.1016/j.jclepro.2019.118857>.
- J. Liu, M. Wu, M. Wang, Simulation of the process for producing butanol from corn fermentation, *Ind. Eng. Chem. Res.* 48 (2009) 5551–5557, <https://doi.org/10.1021/ie900274z>.
- A.B. Van Der Merwe, H. Cheng, J.F. Görgens, J.H. Knoetze, Comparison of energy efficiency and economics of process designs for biobutanol production from sugarcane molasses, *Fuel.* 105 (2013) 451–458, <https://doi.org/10.1016/j.fuel.2012.06.058>.
- W. Van Hecke, E. Joossen-Meyvis, H. Beckers, H. De Wever, Prospects & potential of biobutanol production integrated with organophilic pervaporation – A techno-economic assessment, *Appl. Energy.* 228 (2018) 437–449, <https://doi.org/10.1016/j.apenergy.2018.06.113>.
- A. Oudshoorn, L.A.M. van der Wielen, A.J.J. Straathof, Assessment of options for selective 1-butanol recovery from aqueous solution, *Ind. Eng. Chem. Res.* 48 (2009) 7325–7336, <https://doi.org/10.1021/ie900537w>.
- H.-J. Huang, S. Ramaswamy, Y. Liu, Separation and purification of biobutanol during bioconversion of biomass, *Sep. Purif. Technol.* 132 (2014) 513–540, <https://doi.org/10.1016/j.seppur.2014.06.013>.
- S. van Wyk, A.G.J. van der Ham, S.R.A. Kersten, Pervaporative separation and intensification of downstream recovery of acetone-butanol-ethanol (ABE), *Chem. Eng. Process. - Process Intensif.* 130 (2018) 148–159, <https://doi.org/10.1016/j.cep.2018.06.011>.
- C. Arregoitia-Sarabia, D. González-Revuelta, M. Fallanza, D. Gorri, I. Ortiz, Polymer inclusion membranes containing ionic liquids for the recovery of n-butanol from ABE solutions by pervaporation, *Sep. Purif. Technol.* 248 (2020), 117101, <https://doi.org/10.1016/j.seppur.2020.117101>.
- R. Cabezas, S. Duran, E. Zurob, A. Plaza, G. Merlet, C. Araya-Lopez, J. Romero, E. Quijada-Maldonado, Development of silicone-coated hydrophobic deep eutectic solvent-based membranes for pervaporation of biobutanol, *J. Memb. Sci.* 637 (2021), 119617, <https://doi.org/10.1016/j.memsci.2021.119617>.
- S.S. Hosseini, S. Najari, P.K. Kundu, N.R. Tan, S.M. Roodashti, Simulation and sensitivity analysis of transport in asymmetric hollow fiber membrane permeators for air separation, *RSC Adv.* 5 (2015) 86359–86370, <https://doi.org/10.1039/C5RA13943K>.
- C.Y. Feng, K.C. Khulbe, T. Matsuura, A.F. Ismail, Recent progresses in polymeric hollow fiber membrane preparation, characterization and applications, *Sep. Purif. Technol.* 111 (2013) 43–71, <https://doi.org/10.1016/j.seppur.2013.03.017>.
- H.Z. Chen, Z. Thong, P. Li, T.-S. Chung, High performance composite hollow fiber membranes for CO<sub>2</sub>/H<sub>2</sub> and CO<sub>2</sub>/N<sub>2</sub> separation, *Int. J. Hydrogen Energy.* 39 (2014) 5043–5053, <https://doi.org/10.1016/j.ijhydene.2014.01.047>.
- G. Liu, W. Wei, W. Jin, Pervaporation membranes for biobutanol production, *ACS Sustain. Chem. Eng.* 2 (2014) 546–560, <https://doi.org/10.1021/sc400372d>.
- A. Kujawska, J. Kujawski, M. Bryjak, W. Kujawski, ABE fermentation products recovery methods - A review, *Renew. Sustain. Energy Rev.* 48 (2015) 648–661, <https://doi.org/10.1016/j.rser.2015.04.028>.
- H. Zhu, G. Liu, W. Jin, Recent progress in separation membranes and their fermentation coupled processes for biobutanol recovery, *Energy & Fuels.* 34 (2020) 11962–11975, <https://doi.org/10.1021/acs.energyfuels.0c02680>.
- Y. Wang, N. Widjojo, P. Sukitpaneet, T.-S. Chung, Membrane pervaporation, in: S. Ramaswamy, H.J. Huang, B. V Ramarao (Eds.), *Sep. Purif. Technol. Biorefineries*, John Wiley and Sons, Chichester, West Sussex, United Kingdom, 2013: pp. 259–299. <https://doi.org/10.1002/9781118493441.ch10>.
- A.M. Uriaga, E.D. Gorri, J.K. Beasley, I. Ortiz, Mass transfer analysis of the pervaporative separation of chloroform from aqueous solutions in hollow fiber devices, *J. Memb. Sci.* 156 (1999) 275–291, [https://doi.org/10.1016/S0376-7388\(98\)00350-0](https://doi.org/10.1016/S0376-7388(98)00350-0).
- A. Shepherd, A.C. Habert, C.P. Borges, Hollow fibre modules for orange juice aroma recovery using pervaporation, *Desalination.* 148 (2002) 111–114, [https://doi.org/10.1016/S0011-9164\(02\)00662-8](https://doi.org/10.1016/S0011-9164(02)00662-8).
- K.W. Böddeker, G. Bengtson, H. Pingel, Pervaporation of isomeric butanols, *J. Memb. Sci.* 54 (1990) 1–12, [https://doi.org/10.1016/S0376-7388\(00\)82066-9](https://doi.org/10.1016/S0376-7388(00)82066-9).
- L. Liu, A. Chakma, X. Feng, Preparation of hollow fiber poly(ether block amide)/ polysulfone composite membranes for separation of carbon dioxide from nitrogen, *Chem. Eng. J.* 105 (2004) 43–51, <https://doi.org/10.1016/j.cej.2004.08.005>.
- L. Liu, A. Chakma, X. Feng, Propylene separation from nitrogen by poly(ether block amide) composite membranes, *J. Memb. Sci.* 279 (2006) 645–654, <https://doi.org/10.1016/j.memsci.2005.12.058>.
- Y. Li, J. Shen, K. Guan, G. Liu, H. Zhou, W. Jin, PEBA/ceramic hollow fiber composite membrane for high-efficiency recovery of bio-butanol via pervaporation, *J. Memb. Sci.* 510 (2016) 338–347, <https://doi.org/10.1016/j.memsci.2016.03.013>.
- T.-S. Chung, Y. Feng, *Hollow fiber membranes: Fabrication and applications*, Elsevier, Amsterdam, 2021.
- I. Jesswein, T. Hirth, T. Schiestel, Continuous dip coating of PVDF hollow fiber membranes with PVA for humidification, *J. Memb. Sci.* 541 (2017) 281–290, <https://doi.org/10.1016/j.memsci.2017.07.010>.
- R. Mayank, A. Ranjan, V.S. Moholkar, Mathematical models of ABE fermentation: Review and analysis, *Crit. Rev. Biotechnol.* 33 (2013) 419–447, <https://doi.org/10.3109/07388551.2012.726208>.
- A.M. Uriaga, E.D. Gorri, I. Ortiz, Modeling of the concentration-polarization effects in a pervaporation cell with radial flow, *Sep. Purif. Technol.* 17 (1999) 41–51, [https://doi.org/10.1016/S1383-5866\(99\)00025-8](https://doi.org/10.1016/S1383-5866(99)00025-8).
- V. García, N. Diban, D. Gorri, R. Keiski, A. Uriaga, I. Ortiz, Separation and concentration of bilberry impact aroma compound from dilute model solution by pervaporation, *J. Chem. Technol. Biotechnol.* 83 (2008) 973–982, <https://doi.org/10.1002/jctb.1902>.
- F. Lipnizki, S. Hausmanns, P.K. Ten, R.W. Field, G. Laufenberg, Organophilic pervaporation: Prospects and performance, *Chem. Eng. J.* 73 (1999) 113–129, [https://doi.org/10.1016/S1385-8947\(99\)00024-8](https://doi.org/10.1016/S1385-8947(99)00024-8).
- A. Uriaga, D. Gorri, I. Ortiz, Mass-transfer modeling in the pervaporation of VOCs from diluted solutions, *AIChE J.* 48 (2002) 572–581, <https://doi.org/10.1002/aic.690480314>.
- G. Firpo, E. Angeli, L. Repetto, U. Valbusa, Permeability thickness dependence of polydimethylsiloxane (PDMS) membranes, *J. Memb. Sci.* 481 (2015) 1–8, <https://doi.org/10.1016/j.memsci.2014.12.043>.
- N.N. Li, A.G. Fane, W.S.W. Ho, T. Matsuura, *Advanced membrane technology and applications*, Wiley, Hoboken, N.J., 2008.
- F. Rajaei Gazic, E. Saljoughi, S.M. Mousavi, Recovery of 1-ethyl-2-methylbenzene from wastewater by polymeric membranes via pervaporation process, *J. Polym. Res.* 26 (2019) 272, <https://doi.org/10.1007/s10965-019-1962-7>.
- S. Liu, G. Liu, J. Shen, W. Jin, Fabrication of MOFs/PEBA mixed matrix membranes and their application in bio-butanol production, *Sep. Purif. Technol.* 133 (2014) 40–47, <https://doi.org/10.1016/j.seppur.2014.06.034>.
- A. Selim, K. Knozowska, B. Osmiałowski, J. Kujawa, P. Mizsey, W. Kujawski, The fabrication, characterization, and pervaporation performance of poly(ether-block-amide) membranes blended with 4-(trifluoromethyl)-N(pyridine-2-yl)benzamide and 4-(dimethylamino)-N(pyridine-2-yl)benzamide fillers, *Sep. Purif. Technol.* 268 (2021), 118707, <https://doi.org/10.1016/j.seppur.2021.118707>.
- W. Li, J. Estager, J.-C.-M. Monbaliu, D.P. Debecker, P. Luis, Separation of bio-based chemicals using pervaporation, *J. Chem. Technol. Biotechnol.* 95 (2020) 2311–2334, <https://doi.org/10.1002/jctb.6434>.
- S. Heitmann, V. Krüger, D. Welz, P. Lutze, Experimental investigation of pervaporation membranes for biobutanol separation, *J. Membr. Sep. Technol.* 2 (2013) 245–262.
- F. Liu, L. Liu, X. Feng, Separation of acetone-butanol-ethanol (ABE) from dilute aqueous solutions by pervaporation, *Sep. Purif. Technol.* 42 (2005) 273–282, <https://doi.org/10.1016/j.seppur.2004.08.005>.

- [43] J. Niemistö, W. Kujawski, R.L. Keiski, Pervaporation performance of composite poly(dimethyl siloxane) membrane for butanol recovery from model solutions, *J. Memb. Sci.* 434 (2013) 55–64, <https://doi.org/10.1016/j.memsci.2013.01.047>.
- [44] K. Jirsáková, P. Stanovský, P. Dytrych, L. Morávková, K. Příbylová, Z. Petrusová, J. C. Jansen, P. Izák, Organic vapour permeation in amorphous and semi-crystalline rubbery membranes: Experimental data versus prediction by solubility parameters, *J. Memb. Sci.* 627 (2021), 119211, <https://doi.org/10.1016/j.memsci.2021.119211>.
- [45] P. Li, Y. Chao, Marangoni instability of self-retwetting films modulated by chemical reactions flowing down a vertical fibre, *Chem. Eng. Sci.* 227 (2020), 115936, <https://doi.org/10.1016/j.ces.2020.115936>.
- [46] Y. Abe, Self-retwetting fluids, *Ann. N. Y. Acad. Sci.* 1077 (2006) 650–667, <https://doi.org/10.1196/annals.1362.026>.
- [47] K. Sefiane, X. Yu, G. Duursma, J. Xu, On heat and mass transfer using evaporating self-retwetting mixtures in microchannels, *Appl. Therm. Eng.* 179 (2020), 115662, <https://doi.org/10.1016/j.applthermaleng.2020.115662>.
- [48] A. Talik, M. Tarnacka, M. Geppert-Rybczyńska, B. Hachula, R. Bernat, A. Chrzanowska, K. Kaminski, M. Paluch, Are hydrogen supramolecular structures being suppressed upon nanoscale confinement? The case of monohydroxy alcohols, *J. Colloid Interface Sci.* 576 (2020) 217–229, <https://doi.org/10.1016/j.jcis.2020.04.084>.
- [49] K. Hosseinzadeh, D.D. Ganji, F. Ommi, Effect of SiO<sub>2</sub> super-hydrophobic coating and self-retwetting fluid on two phase closed thermosiphon heat transfer characteristics: An experimental and numerical study, *J. Mol. Liq.* 315 (2020), 113748, <https://doi.org/10.1016/j.molliq.2020.113748>.
- [50] R. Filimonov, Z. Wu, B. Sundén, Toward computationally effective modeling and simulation of droplet formation in microchannel junctions, *Chem. Eng. Res. Des.* 166 (2021) 135–147, <https://doi.org/10.1016/j.cherd.2020.11.010>.
- [51] C. Antonini, F. Villa, I. Bernagozzi, A. Amirfazli, M. Marengo, Drop rebound after impact: The role of the receding contact angle, *Langmuir*. 29 (2013) 16045–16050, <https://doi.org/10.1021/la4012372>.
- [52] L. Guo, Y. Gao, N. Cai, D. Li, Y. Yan, W. Sun, Morphological development of fuel droplets after impacting biomimetic structured surfaces with different temperatures, *J. Bionic Eng.* 17 (2020) 822–834, <https://doi.org/10.1007/s42235-020-0050-3>.
- [53] H.A. Barnes, An examination of the use of rotational viscometers for the quality control on non-newtonian liquid products in factories, *Appl. Rheol.* 11 (2001) 89–101, <https://doi.org/10.1515/arh-2001-0006>.
- [54] J. Franco, D. DeMontigny, S. Kentish, J. Perera, G. Stevens, A study of the mass transfer of CO<sub>2</sub> through different membrane materials in the membrane gas absorption process, *Sep. Sci. Technol.* 43 (2008) 225–244, <https://doi.org/10.1080/01496390701791554>.
- [55] M. Fallanza, A. Ortiz, D. Gorri, I. Ortiz, Using membrane reactive absorption modeling to predict optimum process conditions in the separation of propane-propylene mixtures, *Ind. Eng. Chem. Res.* 52 (2013) 8843–8855, <https://doi.org/10.1021/ie302614r>.
- [56] A. Heintz, W. Stephan, A generalized solution-diffusion model of the pervaporation process through composite membranes. Part II. Concentration polarization, coupled diffusion and the influence of the porous support layer, *J. Memb. Sci.* 89 (1994) 153–169, [https://doi.org/10.1016/0376-7388\(93\)E0223-7](https://doi.org/10.1016/0376-7388(93)E0223-7).
- [57] M.G. Liu, J.M. Dickson, P. Côté, Simulation of a pervaporation system on the industrial scale for water treatment. Part I: Extended resistance-in-series model, *J. Memb. Sci.* 111 (1996) 227–241, [https://doi.org/10.1016/0376-7388\(95\)00234-0](https://doi.org/10.1016/0376-7388(95)00234-0).
- [58] I.F.J. Vankelecom, B. Moermans, G. Verschuere, P.A. Jacobs, Intrusion of PDMS top layers in porous supports, *J. Memb. Sci.* 158 (1999) 289–297, [https://doi.org/10.1016/S0376-7388\(99\)00036-8](https://doi.org/10.1016/S0376-7388(99)00036-8).
- [59] P.V. Naik, R. Bernstein, I.F.J. Vankelecom, Influence of support layer and PDMS coating conditions on composite membrane performance for ethanol/water separation by pervaporation, *J. Appl. Polym. Sci.* 133 (2016) 43670, <https://doi.org/10.1002/app.43670>.
- [60] H. Zeng, S. Liu, J. Wang, Y. Li, L. Zhu, M. Xu, C. Wang, Hydrophilic SPEEK/PES composite membrane for pervaporation desalination, *Sep. Purif. Technol.* 250 (2020), 117265, <https://doi.org/10.1016/j.seppur.2020.117265>.
- [61] W. Gudernatsch, T. Menzel, H. Strathmann, Influence of composite membrane structure on pervaporation, *J. Memb. Sci.* 61 (1991) 19–30, [https://doi.org/10.1016/0376-7388\(91\)80003-0](https://doi.org/10.1016/0376-7388(91)80003-0).
- [62] F. Lipnizki, J. Olsson, P. Wu, A. Weis, G. Trägårdh, R.W. Field, Hydrophobic pervaporation: influence of the support layer of composite membranes on the mass transfer, *Sep. Sci. Technol.* 37 (2002) 1747–1770, <https://doi.org/10.1081/SS-120003042>.
- [63] H. Tan, Y. Wu, T. Li, Pervaporation of n-butanol aqueous solution through ZSM-5-PEBA composite membranes, *J. Appl. Polym. Sci.* 129 (2013) 105–112, <https://doi.org/10.1002/app.38704>.
- [64] S.-Y. Li, R. Srivastava, R.S. Parnas, Separation of 1-butanol by pervaporation using a novel tri-layer PDMS composite membrane, *J. Memb. Sci.* 363 (2010) 287–294, <https://doi.org/10.1016/j.memsci.2010.07.042>.
- [65] W. Liu, S.-L. Ji, H.-X. Guo, J. Gao, Z.-P. Qin, In situ cross-linked-PDMS/BPPO membrane for the recovery of butanol by pervaporation, *J. Appl. Polym. Sci.* 131 (2014), <https://doi.org/10.1002/app.40004>.
- [66] D.L. Vrana, M.M. Meagher, R.W. Hutkins, B. Duffield, Pervaporation of model acetone-butanol-ethanol fermentation product solutions using polytetrafluoroethylene membranes, *Sep. Sci. Technol.* 28 (1993) 2167–2178, <https://doi.org/10.1080/01496399308016741>.
- [67] C. Tong, Y. Bai, J. Wu, L. Zhang, L. Yang, J. Qian, Pervaporation recovery of acetone-butanol from aqueous solution and fermentation broth using HTPB-based polyurethaneurea membranes, *Sep. Sci. Technol.* 45 (2010) 751–761, <https://doi.org/10.1080/01496391003609064>.
- [68] E.A. Fouad, X. Feng, Pervaporative separation of n-butanol from dilute aqueous solutions using silicalite-filled poly(dimethyl siloxane) membranes, *J. Memb. Sci.* 339 (2009) 120–125, <https://doi.org/10.1016/j.memsci.2009.04.038>.
- [69] A. Rozicka, J. Niemistö, R.L. Keiski, W. Kujawski, Apparent and intrinsic properties of commercial PDMS based membranes in pervaporative removal of acetone, butanol and ethanol from binary aqueous mixtures, *J. Memb. Sci.* 453 (2014) 108–118, <https://doi.org/10.1016/j.memsci.2013.10.065>.
- [70] J. Kujawski, A. Rozicka, M. Bryjak, W. Kujawski, Pervaporative removal of acetone, butanol and ethanol from binary and multicomponent aqueous mixtures, *Sep. Purif. Technol.* 132 (2014) 422–429, <https://doi.org/10.1016/j.seppur.2014.05.047>.
- [71] I.L. Borisov, A.O. Malakhov, V.S. Khotimsky, E.G. Litvinova, E.S. Finkelshtein, N. V. Ushakov, V.V. Volkov, Novel PTMSP-based membranes containing elastic filler: Enhanced 1-butanol/water pervaporation selectivity and permeability, *J. Memb. Sci.* 466 (2014) 322–330, <https://doi.org/10.1016/j.memsci.2014.04.037>.
- [72] A.G. Fadeev, Y. Selinskaya, S.S. Kelley, M.M. Meagher, E.G. Litvinova, V. S. Khotimsky, V.V. Volkov, Extraction of butanol from aqueous solutions by pervaporation through poly(1-trimethylsilyl-1-propyne), *J. Memb. Sci.* 186 (2001) 205–217, [https://doi.org/10.1016/S0376-7388\(00\)00683-9](https://doi.org/10.1016/S0376-7388(00)00683-9).
- [73] C. Xue, G.-Q. Du, L.-J. Chen, J.-G. Ren, F.-W. Bai, Evaluation of asymmetric polydimethylsiloxane-polyvinylidene fluoride composite membrane and incorporated with acetone-butanol-ethanol fermentation for butanol recovery, *J. Biotechnol.* 188 (2014) 158–165, <https://doi.org/10.1016/j.jbiotec.2014.08.010>.
- [74] J. Kujawa, S. Cerneaux, W. Kujawski, Removal of hazardous volatile organic compounds from water by vacuum pervaporation with hydrophobic ceramic membranes, *J. Memb. Sci.* 474 (2015) 11–19, <https://doi.org/10.1016/j.memsci.2014.08.054>.